Available online at www.sciencedirect.com

SCIENCE DIRECT®

International Journal of Solids and Structures 43 (2006) 5541–5554

INTERNATIONAL JOURNAL OF SOLIDS and STRUCTURES

www.elsevier.com/locate/ijsolstr

Piezoelastic study on singularities interacting with circular and straight interfaces

F.M. Chen, M.H. Shen *, S.N. Chen

Department of Mechanical Engineering, Nan Kai Institute of Technology, 568 Chung Cheng Road, Tsao Tun, 542, Nantou County, Taiwan

Received 3 May 2005; received in revised form 9 June 2005
Available online 15 August 2005

Abstract

The piezoelastic investigation for a circular inclusion embedded in a sandwich has been carried out. Each medium of the composite is assumed to be transversely isotropic with hexagonal symmetry, which has an isotropic basal plane of x_1x_2-plane and a poling direction of x_3-axis. The electromechanical loadings considered in this paper include a point force and a point charge located in the middle layer of the sandwich. An efficient procedure is established by combining the analytical continuation method and alternating technique to derive the general forms of the piezoelastic fields in terms of the corresponding problem. Numerical results are provided for a number of particular examples to study the influence of material combinations, geometry, and loading condition on both the mechanical and electric response.

Keywords: Electromechanical loadings; Analytical continuation; Alternating technique

1. Introduction

There has been an explosion of interest in the field of piezoelectric materials in recent years. The electromechanical response of piezoelectric materials is complex as it involves a mechanical response, an electrical response, and a mutual coupling between the mechanical and electrical domains. Due to the intrinsic electro-mechanical coupling behavior, piezoelectric materials have been widely used in various fields, such as actuators, transducers, sensors and more. In order to predict the performance and integrity of these devices, it is important that the behavior of various defects such as cracks, dislocations and inclusions are analyzed and studied under the electrical and mechanical fields.

* Corresponding author. Tel.: +886 49 2563489x3412; fax: +886 49 2565674.
E-mail address: mhshen@nkc.edu.tw (M.H. Shen).

0020-7683/$ - see front matter
doi:10.1016/j.ijsolstr.2005.06.052

Numerous attempts have been made to analyze the inclusion problems in piezoelectric materials, see for example the works of Pak (1992), Honein et al. (1995), Zhong and Meguid (1997), Weichen (1997), Meguid and Deng (1998), Xiao and Bai (1999a,b), Liu et al. (2000), Wang and Shen (2001), Huang and Kuang (2001), Jiang and Cheung (2001), among others. Based on the complex variable theory in conjunction with the Möebius transformation, Chao and Chang (1999) studied the problem of multiple piezoelectric circular inclusions embedded in an infinite matrix. By using the alternating technique and analytical continuation method, Chen et al. (2004) solved a piezoelastic singularity problem of a trimaterial composed of three dissimilar materials bonded along two parallel interfaces. However, for a piezoelectric media with more than two straight or circular interfaces, mathematical difficulties are encountered. To our knowledge, the electroelastic behavior of a circular inclusion embedded in a plane layered media subjected to point electromechanical singularities has not been studied yet.

In the present study, we focus on the derivation of the analytical model of a circular inclusion embedded in the middle layer of the sandwich which is subjected to a point force and point charge. The proposed method is based upon the technique of analytical continuation that is alternatively applied across each interface in order to derive the complex potentials for each component of the composite in a series form from the corresponding homogeneous solution.

This paper is divided into six sections. Following this brief introduction, a complex representation of piezoelectricity is provided in Section 2, the solution of singularities problem of a bi-material is provided in Section 3, and the alternating technique together with the results of Section 3 is employed to derive the solution of the multiple-phase media in Section 4. Numerical results are presented graphically for some particular cases in Section 5 and finally we conclude the current article in Section 6.

2. A complex representation of anti-plane piezoelectricity

Consider a piezoelectric system composed of a dissimilar circular inclusion embedded in the middle layer of three-phase sandwich as depicted in Fig. 1. Each component is assumed to be transversely isotropic with hexagonal symmetry and poled along the-x_3 direction with an isotropic $0x_1x_2$-plane. In a class of piezoelectric materials capable of undergoing out-of-plane displacement u_3 and in-plane electric potential ϕ, the only non-vanishing components of the stress field, the electric field and the electric displacement are given by

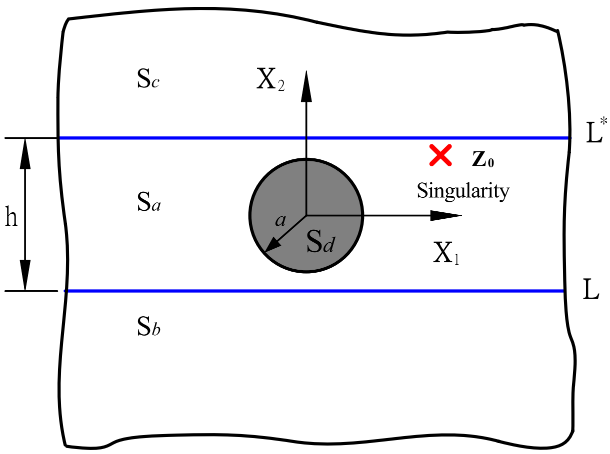

Fig. 1. A circular inclusion in a sandwich with a singularity in the middle layer.

$$\sigma_{13} = \sigma_{31} = c_{44}\frac{\partial u_3}{\partial x_1} + e_{15}\frac{\partial \phi}{\partial x_1} \tag{1}$$

$$\sigma_{23} = \sigma_{32} = c_{44}\frac{\partial u_3}{\partial x_2} + e_{15}\frac{\partial \phi}{\partial x_2} \tag{2}$$

$$E_1 = -\frac{\partial \phi}{\partial x_1} \tag{3}$$

$$E_2 = -\frac{\partial \phi}{\partial x_2} \tag{4}$$

$$D_1 = e_{15}\frac{\partial u_3}{\partial x_1} - \varepsilon_{11}\frac{\partial \phi}{\partial x_1} \tag{5}$$

$$D_2 = e_{15}\frac{\partial u_z}{\partial x_2} - \varepsilon_{11}\frac{\partial \phi}{\partial x_2} \tag{6}$$

It is convenient to use a complex representation for u_3 and ϕ which are grouped as a vector.

$$\mathrm{Re}[\mathbf{U}] = \begin{Bmatrix} u_3 \\ \phi \end{Bmatrix} \tag{7}$$

where Re denotes the real part of a complex function and $\mathbf{U}$ is the generalized displacement with two components being holomorphic functions. The components of the stress and electric displacement are related to the generalized displacement by

$$\begin{Bmatrix} \sigma_{31} - \mathrm{i}\sigma_{32} \\ D_1 - \mathrm{i}D_2 \end{Bmatrix} = \begin{bmatrix} c_{44} & e_{15} \\ e_{15} & -\varepsilon_{11} \end{bmatrix}\mathbf{U}' = \mathbf{C}\mathbf{U}' \tag{8}$$

where prime indicates differentiation with respect to the complex variable $z = x_1 + \mathrm{i}x_2$.

In order to express the boundary condition in terms of $\mathbf{U}$ rather than its derivative $\mathbf{U}'$, we take an integration of the traction t and normal electric displacement D_n as

$$\int \begin{Bmatrix} t \\ D_n \end{Bmatrix} \mathrm{d}s = \mathrm{Im}[\mathbf{C}\mathbf{U}] \tag{9}$$

where $[\,t \quad D_n\,]^{\mathrm{T}}$ is referred to as the generalized traction and Im denotes the imaginary part of a complex function.

3. A singularity in a bi-material

3.1. A bi-material composed of two half plane

The solution of a singularity in a bi-piezoelectric material bonded along x_1-axis (see Fig. 2) is constructed by the method of analytical continuation in terms of the homogeneous solution $\mathbf{U}_0(z)$. Where S_a, the upper half-space, and S_b, the lower half-space, are occupied by material a and b, respectively. If the singularity located in lower half-space ($z \in S_b$), in which the material constants of material b are implied in $\mathbf{U}_0(z)$. The continuities of Re[U] and Im[CU] across the interface are used to determine the bi-material solution. By the analytical continuation method, one can obtain

$$\begin{cases} \mathbf{U}_a(z) = \boldsymbol{\alpha}_{ab}\mathbf{U}_0(z) & z \in S_a \\ \mathbf{U}_b(z) = \mathbf{U}_0(z) + \boldsymbol{\beta}_{ab}\overline{\mathbf{U}}_0(z) & z \in S_b \end{cases} \tag{10}$$

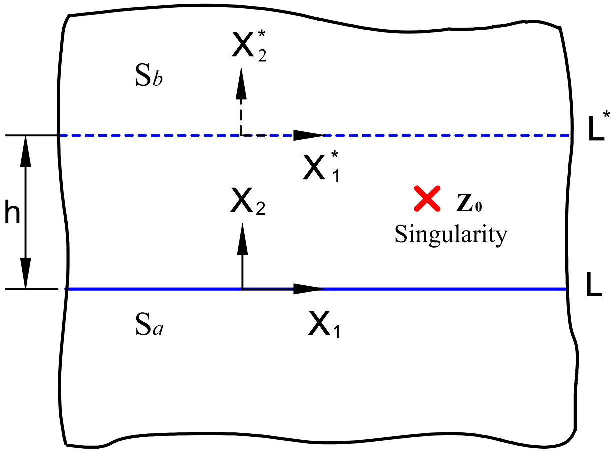

Fig. 2. A singularity in a bi-material.

where

$$\mathbf{C}_a = \begin{bmatrix} c_{44}^{(a)} & e_{15}^{(a)} \\ e_{15}^{(a)} & -\varepsilon_{11}^{(a)} \end{bmatrix}$$
$$\mathbf{C}_b = \begin{bmatrix} c_{44}^{(b)} & e_{15}^{(b)} \\ e_{15}^{(b)} & -\varepsilon_{11}^{(b)} \end{bmatrix}$$
$$\boldsymbol{\alpha}_{ab} = 2(\mathbf{C}_a + \mathbf{C}_b)^{-1}\mathbf{C}_b$$
$$\boldsymbol{\beta}_{ab} = (\mathbf{C}_a + \mathbf{C}_b)^{-1}(\mathbf{C}_b - \mathbf{C}_a)$$

For a singularity located in the upper half-space, by the same procedure, the solution is found to be

$$\begin{cases} \mathbf{U}_a(z) = \mathbf{U}_0(z) + \boldsymbol{\beta}_{ba}\overline{\mathbf{U}_0}(z) & z \in S_a \\ \mathbf{U}_b(z) = \boldsymbol{\alpha}_{ba}\mathbf{U}_0(z) & z \in S_b \end{cases} \tag{11}$$

3.2. A coordinate translation

Suppose that regions $S_a{:}x_2 \geqslant h$ and $S_b{:}x_2 \leqslant h$ occupied by material a and b, respectively, are perfectly bonded along the interface $x_2 = h$. With a coordinate translation $z^* = z - \mathrm{i}h$, (see Fig. 2), it is easy to show that the generalized displacement $\mathbf{U}$(z) in the x_1x_2 coordinate system is related to the function $\mathbf{U}^*(z^*)$ in the $x_1^*x_2^*$ coordinate system by Suo (1989)

$$\mathbf{U}^*(z^*) = \mathbf{U}(z), \quad \overline{\mathbf{U}^*}(z^*) = \overline{\mathbf{U}}(z - 2\mathrm{i}h) \tag{12}$$

3.3. A circular inclusion embedded in an infinite plane

Consider a circular inclusion embedded in an infinite plane which is subjected to a singularity as shown in Fig. 3 where S_a, the inner region, and S_b, the outer region, are occupied by material a and material b,

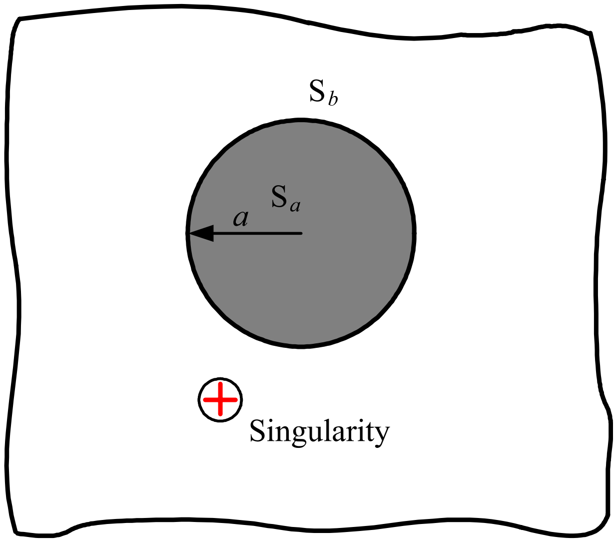

Fig. 3. A circular inclusion embedded in an infinite plane.

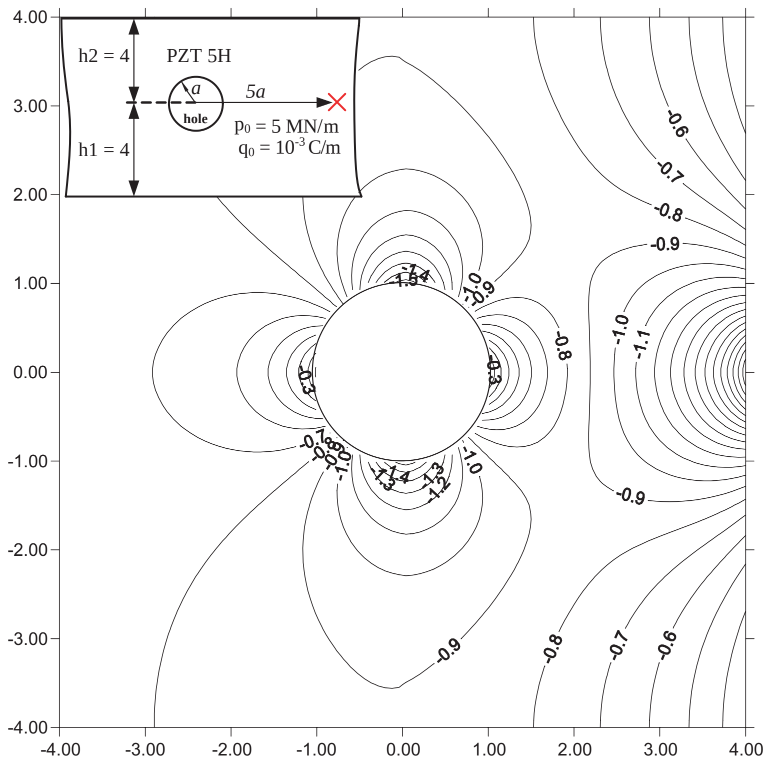

Fig. 4. Contours of constant normalized electric field $E_1a/q_0\varepsilon_{11}^a$.

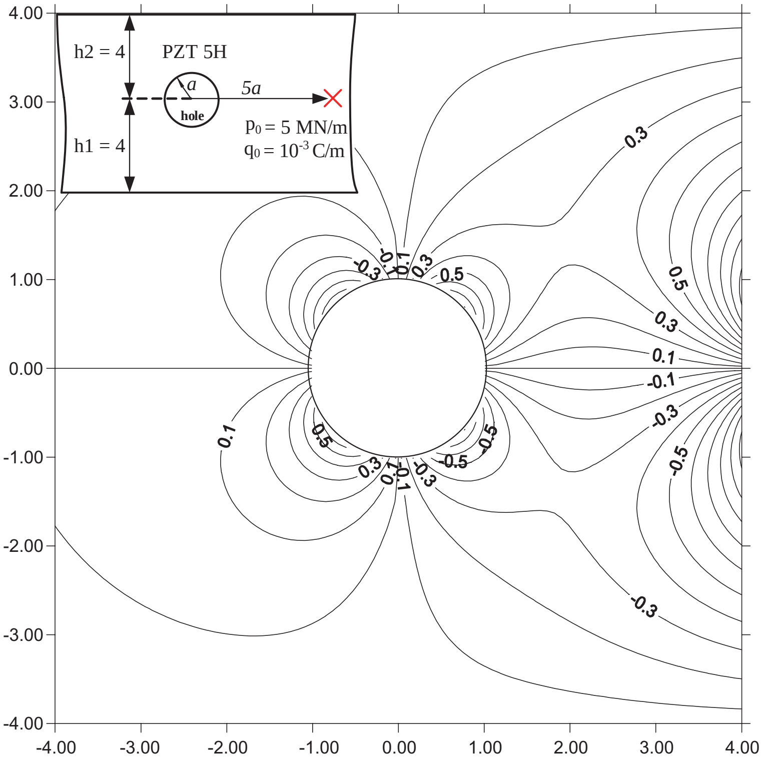

Fig. 5. Contours of constant normalized electric field $E_2a/q_0\varepsilon_{11}^a$.

respectively. The continuities of Re[**U**] and Im[**CU**] across the interface are used to determine the bi-material solution. By analytical continuation method, one can obtain

$$\begin{cases} \boldsymbol{\alpha}_{ab}\mathbf{U}_0(z) & z \in S_a \\ \mathbf{U}_0(z) + \boldsymbol{\beta}_{ab}\overline{\mathbf{U}}_0(\frac{a^2}{z}) & z \in S_b \end{cases} \tag{13}$$

4. A singularity in a multiple-phase media

The alternating technique together with the results of the previous sections can be employed to analyze a singularity in a multiple-phase media (Fig. 1). Since it is difficult to satisfy the continuity conditions along all interfaces at the same time, the method of analytical continuation should be applied to each interface alternatively. Assume a series solution for the case of the singularity located in S_a as

$$\begin{cases} \mathbf{U}_a(z) = \mathbf{U}_0(z) + \sum_{n=1}^{\infty} \mathbf{U}_{an}(z) \\ \mathbf{U}_b(z) = \sum_{n=1}^{\infty} \mathbf{U}_{bn}(z) \\ \mathbf{U}_c(z) = \sum_{n=1}^{\infty} \mathbf{U}_{cn}(z) \\ \mathbf{U}_d(z) = \sum_{n=1}^{\infty} \mathbf{U}_{dn}(z) \end{cases} \tag{14}$$

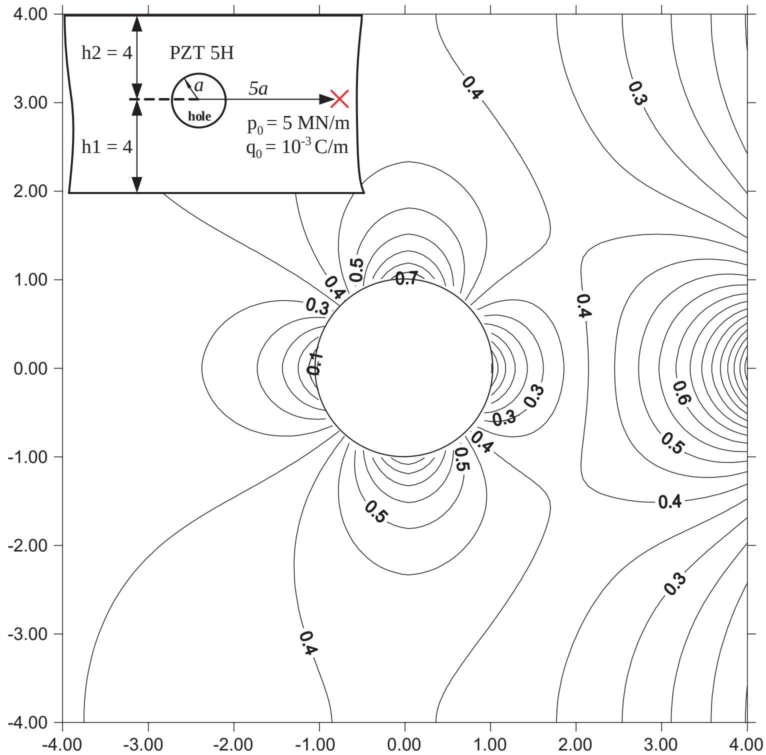

Fig. 6. Contours of constant normalized shear stress $\sigma_{31}a/p_0$.

where $\mathbf{U}_{an}(z)$, $\mathbf{U}_{bn}(z)$, $\mathbf{U}_{cn}(z)$ and $U_{dn}(z)$ are holomorphic functions in their respective region. Since the middle layer is bonded with each other medium, we first assume $U_{j1}(z)$ $(j = a, b, c, d)$ by putting all bi-material solutions together in $U_{a1}(z)$ as

$$\begin{cases} \mathbf{U}_{a1}(z) = \boldsymbol{\beta}_{ba}\overline{\mathbf{U}_0}(A_bz) + \boldsymbol{\beta}_{ca}\overline{\mathbf{U}_0}(A_cz) + \boldsymbol{\beta}_{da}\overline{\mathbf{U}_0}(A_dz) \\ \mathbf{U}_{b1}(z) = \boldsymbol{\alpha}_{ba}\mathbf{U}_0(z) \\ \mathbf{U}_{c1}(z) = \boldsymbol{\alpha}_{ca}\mathbf{U}_0(z) \\ \mathbf{U}_{d1}(z) = \boldsymbol{\alpha}_{da}\mathbf{U}_0(z) \end{cases} \tag{15}$$

where A_bz, A_cz and A_dz represent the transformation functions defined as

$$A_bz = z + 2\mathrm{i}h$$
$$A_cz = z - 2\mathrm{i}h$$
$$A_dz = \frac{a^2}{z}$$

Obviously, the above equations cannot satisfy the continuity conditions across all interfaces since $\mathbf{U}_{a1}(z)$ contains two superfluous terms for each interface. For example, the first and second terms of $\mathbf{U}_{a1}(z)$ cannot satisfy the continuity conditions at L_d, the second and third terms of $\mathbf{U}_{a1}(z)$ cannot satisfy the continuity conditions at L_b, and the first and third terms of $\mathbf{U}_{a1}(z)$ cannot satisfy the continuity conditions at L_a.

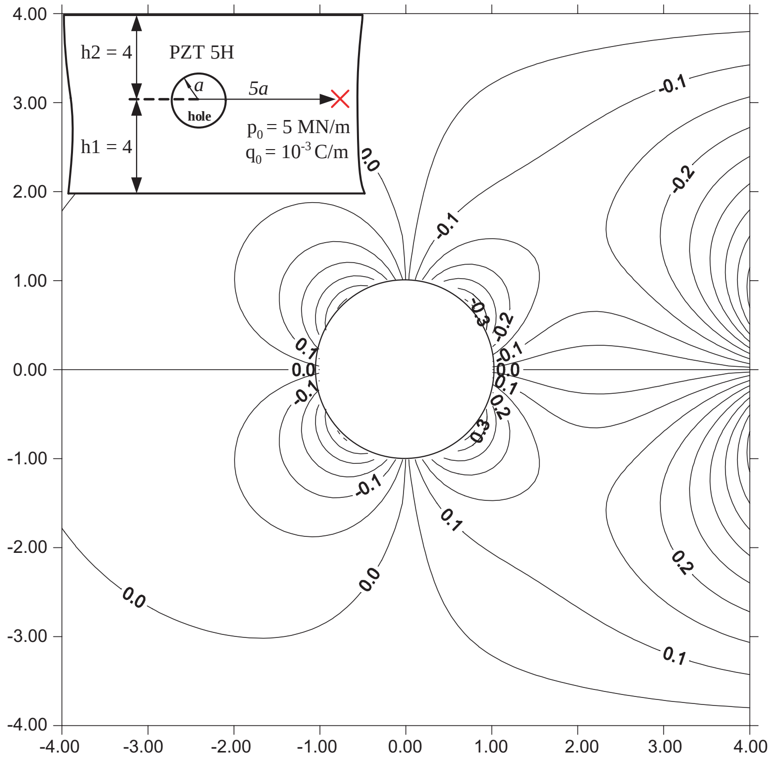

Fig. 7. Contours of constant normalized shear stress $\sigma_{32}a/p_0$.

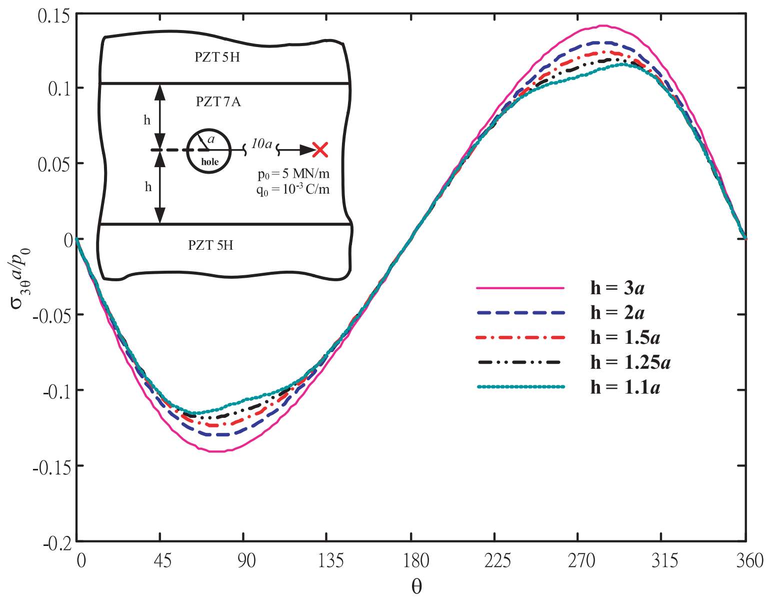

Fig. 8. Angular variations of the tangential shear stress along the circular hole in a sandwich.

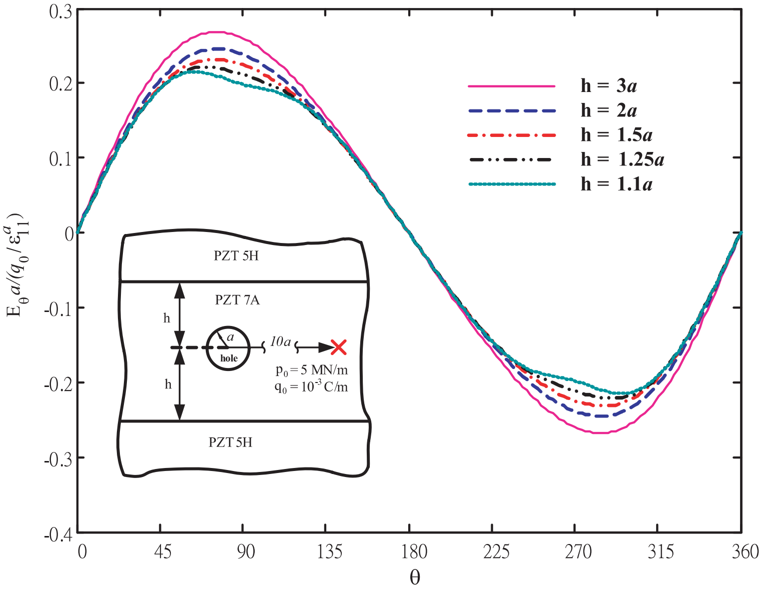

Fig. 9. Angular variations of the interfacial tangential electric field along the circular hole in a sandwich.

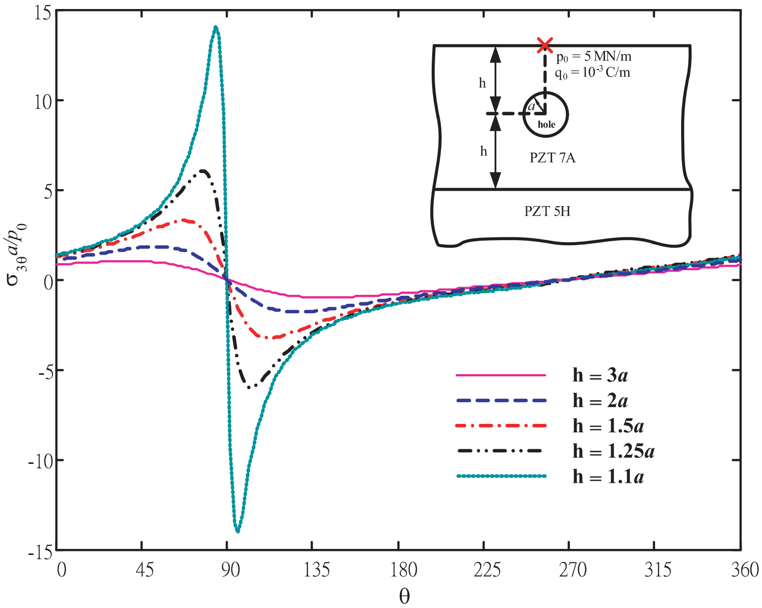

Fig. 10. Angular variations of the tangential shear stress along the circular hole in a film/substrate structure.

To let the superfluous terms of $\mathbf{U}_{a1}(z)$ for each interface to satisfy the continuity conditions, additional terms $\mathbf{U}_{a2}(z)$, $\mathbf{U}_{b2}(z)$, $\mathbf{U}_{c2}(z)$ and $\mathbf{U}_{d2}(z)$ holomorphic in S_a, S_b, S_c and S_d, respectively should be introduced to satisfy the continuity conditions across all interfaces, the method of analytical continuation is applied to all interfaces alternatively to obtain

$$\begin{cases} \mathbf{U}_{a2}(z) = \boldsymbol{\beta}_{ba}\boldsymbol{\beta}_{ca}\mathbf{U}_0(\overline{A}_c A_b z) + \boldsymbol{\beta}_{ba}\boldsymbol{\beta}_{da}\mathbf{U}_0(\overline{A}_d A_b z) + \boldsymbol{\beta}_{ca}\boldsymbol{\beta}_{ba}(\overline{A}_b A_c z) \\ \qquad\qquad + \boldsymbol{\beta}_{ca}\boldsymbol{\beta}_{da}\mathbf{U}_0(\overline{A}_d A_c z) + \boldsymbol{\beta}_{da}\boldsymbol{\beta}_{ba}\mathbf{U}_0(\overline{A}_b A_d z) + \boldsymbol{\beta}_{da}\boldsymbol{\beta}_{ca}\mathbf{U}_0(\overline{A}_c A_d z) \\ \mathbf{U}_{b2}(z) = \boldsymbol{\alpha}_{ba}[\boldsymbol{\beta}_{ca}\overline{\mathbf{U}_0}(A_c z) + \boldsymbol{\beta}_{da}\overline{\mathbf{U}_0}(A_d z)] \\ \mathbf{U}_{c2}(z) = \boldsymbol{\alpha}_{ca}[\boldsymbol{\beta}_{ba}\overline{\mathbf{U}_0}(A_b z) + \boldsymbol{\beta}_{da}\overline{\mathbf{U}_0}(A_d z)] \\ \mathbf{U}_{d2}(z) = \boldsymbol{\alpha}_{da}[\boldsymbol{\beta}_{ba}\overline{\mathbf{U}_0}(A_b z) + \boldsymbol{\beta}_{ca}\overline{\mathbf{U}_0}(A_c z)] \end{cases} \tag{16}$$

But it is clear that $\mathbf{U}_{a2}(z)$ still contains four superfluous terms to satisfy the continuity conditions at each interface. The previous procedure should be repeated to get the results of which the continuity conditions are satisfied at all interfaces as follow:

$$\begin{cases} \mathbf{U}_{an}(z) = \boldsymbol{\beta}_{ba}[\overline{\mathbf{U}}^c_{a(n-1)}(A_c z) + \overline{\mathbf{U}}^d_{a(n-1)}(A_d z)] \\ \qquad\qquad + \boldsymbol{\beta}_{ca}[\overline{\mathbf{U}}^b_{a(n-1)}(A_b z) + \overline{\mathbf{U}}^d_{a(n-1)}(A_d z)] \\ \qquad\qquad + \boldsymbol{\beta}_{ba}[\overline{\mathbf{U}}^b_{a(n-1)}(A_b z) + \overline{\mathbf{U}}^c_{a(n-1)}(A_c z)] \quad \text{for } n = 3, 4, 5 \ldots \\ \mathbf{U}_{bn}(z) = \boldsymbol{\alpha}_{ba}[\mathbf{U}^c_{a(n-1)}(z) + \mathbf{U}^d_{a(n-1)}(z)] \\ \mathbf{U}_{cn}(z) = \boldsymbol{\alpha}_{ca}[\mathbf{U}^b_{a(n-1)}(z) + \mathbf{U}^d_{a(n-1)}(z)] \\ \mathbf{U}_{dn}(z) = \boldsymbol{\alpha}_{da}[\mathbf{U}^b_{a(n-1)}(z) + \mathbf{U}^c_{a(n-1)}(z)] \end{cases} \tag{17}$$

where

$$\mathbf{U}^b_{a(n-1)}(z) = \boldsymbol{\beta}_{ca}\overline{\mathbf{U}}_{a(n-2)}(A_c z) + \boldsymbol{\beta}_{da}\overline{\mathbf{U}}_{a(n-2)}(A_d z) \tag{18}$$

$$\mathbf{U}^c_{a(n-1)}(z) = \boldsymbol{\beta}_{ba}\overline{\mathbf{U}}_{a(n-2)}(A_b z) + \boldsymbol{\beta}_{da}\overline{\mathbf{U}}_{a(n-2)}(A_d z) \tag{19}$$

$$\mathbf{U}^d_{a(n-1)}(z) = \boldsymbol{\beta}_{ba}\overline{\mathbf{U}}_{a(n-2)}(A_b z) + \boldsymbol{\beta}_{da}\overline{\mathbf{U}}_{c(n-2)}(A_c z) \tag{20}$$

For the problem of a three-layer composite subjected to a singularity in the middle layer with thickness being h (see Fig. 7), by letting material d be made of material a and with the same procedure, Eq. (14) can be simplified to the following explicit form:

$$\begin{cases} \mathbf{U}_a(z) = \sum_{n=0}^{\infty}(\boldsymbol{\beta}_{ba}\boldsymbol{\beta}_{ca})^n\left[\mathbf{U}_0(z + 2ni h) + \boldsymbol{\beta}_{ba}\overline{\mathbf{U}_0}(z + 2ni h)\right] \\ \qquad\qquad + \boldsymbol{\beta}_{ca}\sum_{n=1}^{\infty}(\boldsymbol{\beta}_{ba}\boldsymbol{\beta}_{ca})^{n-1}\left[\overline{\mathbf{U}_0}(z - 2ni h) + \boldsymbol{\beta}_{ba}\mathbf{U}_0(z - 2ni h)\right] \\ \mathbf{U}_b(z) = \boldsymbol{\alpha}_{ba}\mathbf{U}_0(z) + \boldsymbol{\alpha}_{ba}\beta_{ca}\sum_{n=1}^{\infty}(\boldsymbol{\beta}_{ba}\boldsymbol{\beta}_{ca})^{n-1}\left[\overline{\mathbf{U}_0}(z - 2ni h) + \boldsymbol{\beta}_{ba}\mathbf{U}_0(z - 2ni h)\right] \\ \mathbf{U}_c(z) = \boldsymbol{\alpha}_{ca}\sum_{n=0}^{\infty}(\boldsymbol{\beta}_{ba}\boldsymbol{\beta}_{ca})^n\left[\mathbf{U}_0(z + 2ni h) + \boldsymbol{\beta}_{ba}\overline{\mathbf{U}_0}(z + 2ni h)\right] \end{cases} \tag{21}$$

which is in agreement with the result provided by Chen et al. (2004).

5. Results and discussion

In this section, we provide four particular examples to study the influence of material combinations, geometric configuration, and loading conditions on both the mechanical and electric response. The composite of these examples is made up of two commonly used piezoelectric ceramics PZT-5H and PZT-7A with material constants $c_{44} = 35.3\ \mathrm{GNm}^{-2}$, $\varepsilon_{11} = 15.1\ \mathrm{nCV}^{-1}\,\mathrm{m}^{-1}$, $e_{15} = 17\ \mathrm{Cm}^{-2}$ and $c_{44} = 25.4\ \mathrm{GNm}^{-2}$,

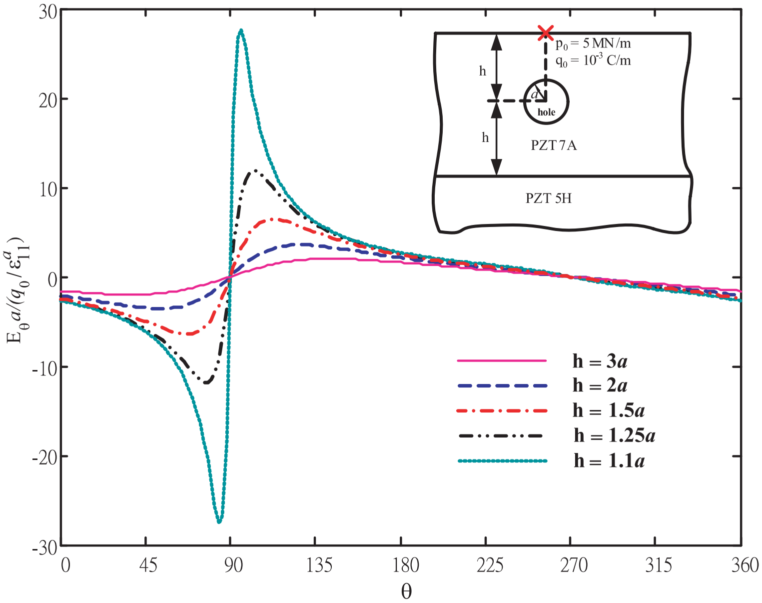

Fig. 11. Angular variations of the interfacial tangential electric field along the circular hole in a film/substrate structure.

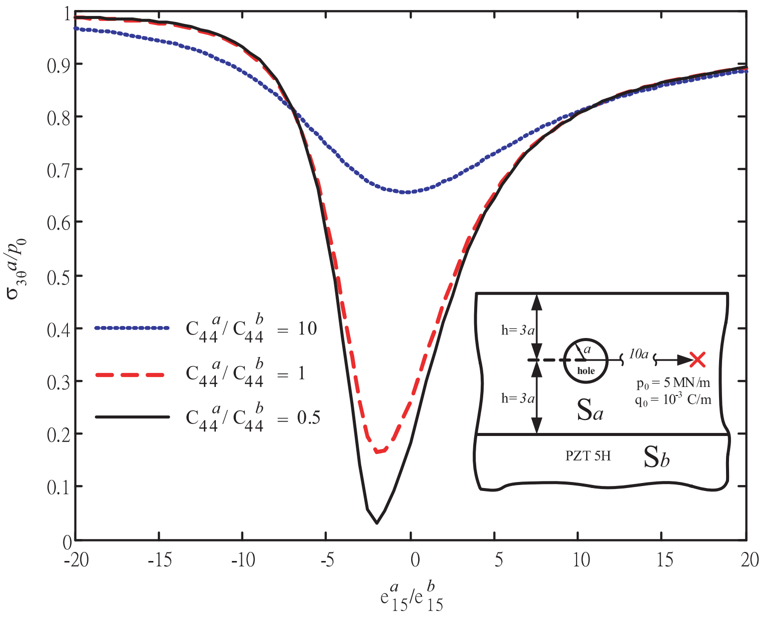

Fig. 12. Variations of tangential shear stress vs. the piezoelectric constant ratios for a film/substrate structure.

$\varepsilon_{11} = 4.071\ \text{nCV}^{-1}\,\text{m}^{-1}$, $e_{15} = 9.2\ \text{Cm}^{-2}$, respectively. Besides, the piezoelectric constants of the air are assumed as $c_{44} = 0$, $\varepsilon_{11} = 8.85\ \text{nCV}^{-1}\,\text{m}^{-1}$, $e_{15} = 0\ \text{Cm}^{-2}$ in the following discussion.

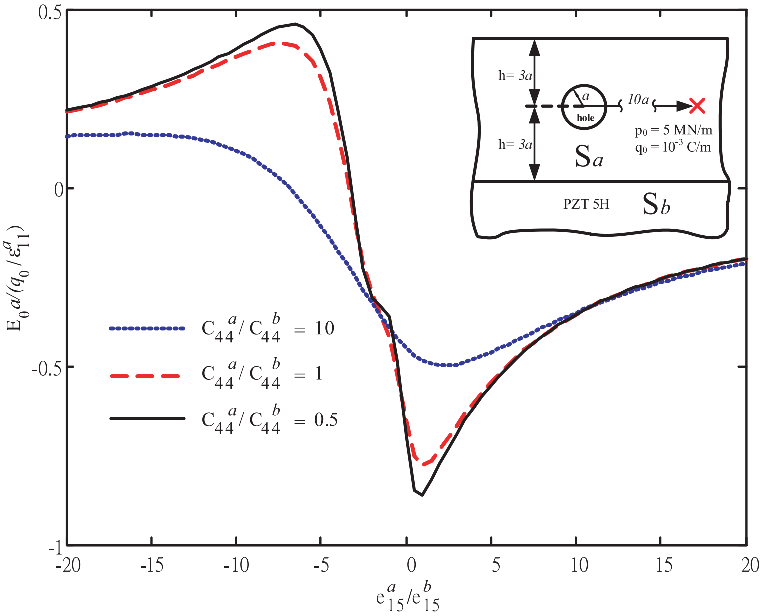

Fig. 13. Variations of tangential electric field vs. the piezoelectric constant ratios for a film/substrate structure.

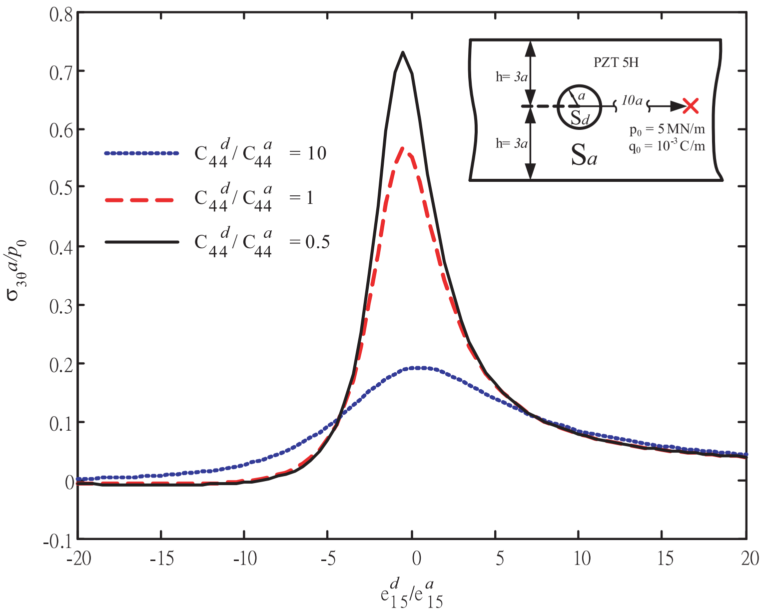

Fig. 14. Variations of tangential shear stress vs. the piezoelectric constant ratios for a circular inclusion in a strip.

As our first example, we consider a PZT-5H strip containing a circular hole subjected to a point force and a point charge. Figs. 4 and 5, respectively show contours of constant normalized electric fields $E_1 a/q_0\varepsilon_{11}^a$ and $E_2 a/q_0\varepsilon_{11}^a$ due to a point electromechanical loadings. From these figures one can observe

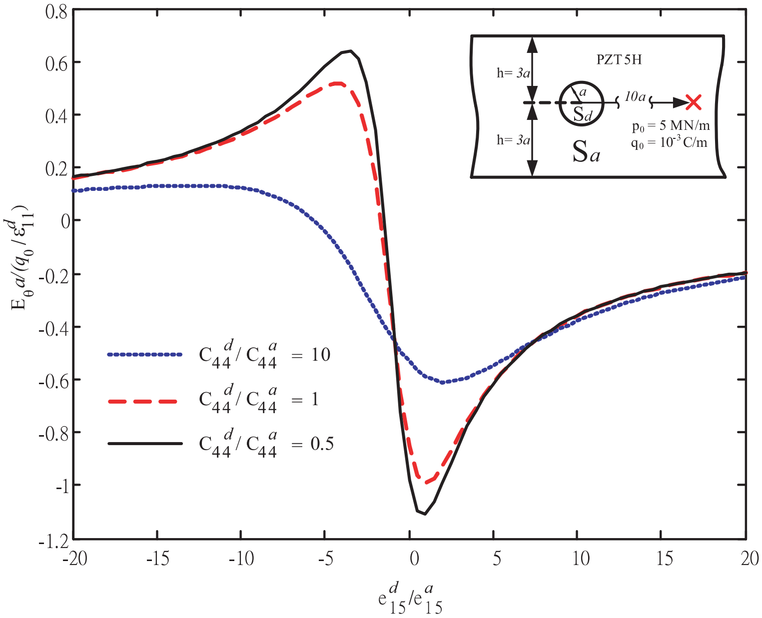

Fig. 15. Variations of tangential electric field vs. the piezoelectric constant ratios for a circular inclusion in a strip.

the difference between contours of the electric fields as a result of the applied anti-plane mechanical and in-plane electric loadings. Although severe concentrations are observed about the point of the singularity and the boundary of the hole in both cases, the contour shape in these two plots is quite different. For example, $E_1a/q_0\varepsilon_{11}^a$ is symmetric about x_1-axis as shown in Fig. 4, while $E_2a/q_0\varepsilon_{11}^a$ is anti-symmetric about the x_1-axis as shown in Fig. 5. Figs. 6 and 7, respectively show contours of constant normalized shear stresses $\sigma_{31}a/p_0$ and $\sigma_{32}a/p_0$ due to point electromechanical loadings. Similarly, although severe concentrations are observed about the point of the singularity and the boundary of the hole in both cases, the contour shape in these two figures is quite different. For example, $\sigma_{31}a/p_0$ is symmetric about the x_1-axis as shown in Fig. 6, while $\sigma_{32}a/p_0$ is anti-symmetric about the x_1-axis as shown in Fig. 7. For a second example, we consider a circular hole in the middle layer of a sandwich. Figs. 8 and 9, respectively show the angular variations of the tangential shear stress and electric field along the circular hole. One can observe that both the magnitude of the tangential shear stress and electric field increase with increasing h/a ratio. As a third example, we consider a film/substrate structure with a hole in the film which is subjected to a point force and a point charge. Figs. 10 and 11, respectively show the angular variations of the tangential shear stress and electric field along the circular hole. We can observe that both the tangential shear stress and electric field along the circular hole experience a big jump across the point $\theta = 90°$ which is nearest to the applied point singularity approach the circular hole, and both the maximum magnitude of tangential shear stress and electric field increase with decreasing h/a ratio. Figs. 12 and 13 display the distribution of shear stress and electric field at the point $z = ai$ as a function of the piezoelectric constant ratios, respectively. One can observe that both the maximum magnitude of the shear stress and electric field decrease with the elastic modulus of the film. As our fourth example, we consider a circular inclusion embedded in a PZT-5H strip. The material constants of the inclusion are assumed as the same of the strip except the piezoelectric constant. Figs. 14 and 15 display the distribution of shear stress and electric field at the point $z = ai$ as a function of the piezoelectric constant ratios, respectively. One can observe that both the maximum magnitude of the electric field and shear stress decrease with the elastic modulus of the inclusion. This phenomenon is helpful for us to build a more effective sensor and active actuator.

6. Conclusion

An efficient procedure for solving a circular inclusion embedded in a sandwich subjected to a point electro-elastic singularity is established. Compared to the three-phase multiplying region problem, more mathematical difficulties are encountered in this study. Since one of the medium is connected with each other medium, a particular treatment of combining the analytical continuation method and alternating technique is applied to derive the general series solutions for the piezoelectric fields in each medium explicitly. It was shown that both the stress and electric fields are dependent on the mismatch of the material constants, the geometric parameter of the system and electromechanical loading conditions. Moreover, this approach could lead to some interesting simplifications in solution procedure and the derived analytical solution can be employed as Green's function to investigate the corresponding crack problems.

References

Chao, C.K., Chang, K.J., 1999. Interacting circular inclusions in antiplane piezoelectricity. International Journal of Solids and Structures 36, 3349–3373.

Chen, F.M., Shen, M.H., Lin, Y.J., 2004. Anti-plane piezoelastic study on singularities interacting with interfaces. International Journal of Mechanical Sciences 46, 1459–1470.

Honein, E., Honein, T., Herrmann, G., 1995. On the interaction of two piezoelectric fibers embedded in an intelligent material. Journal of Intelligent Material Systems and Structures 6, 229–236.

Huang, Z., Kuang, Z.B., 2001. Dislocation inside a piezoelectric media with an elliptical inhomogeneity. International Journal of Solids and Structures 38, 8459–8480.

Jiang, C.P., Cheung, Y.K., 2001. An exact solution for the three-phase piezoelectric cylinder model under antiplane shear and its applications to piezoelectric composites. International Journal of Solids and Structures 38, 4777–4796.

Liu, J.X., Jiang, Z.Q., Feng, W.J., 2000. On the electro-elastic interaction of piezoelectric screw dislocation with an elliptical inclusion in piezoelectric materials. Applied Mathematics and Mechanics 21, 1185–1190.

Meguid, S.A., Deng, W., 1998. Electro-elastic interaction between a screw dislocation and elliptical inhomogeneity in piezoelectric materials. International Journal Solids and Structures 35, 1467–1482.

Pak, Y.E., 1992. Circular inclusion problem in anti-plane piezoelectricity. International Journal of Solids and Structures 29, 2403–2419.

Suo, Z., 1989. Singularities interacting with interfaces and cracks. International Journal of Solids and Structures 25, 1133–1142.

Wang, X., Shen, Y.P., 2001. On double circular inclusion problem in antiplane piezoelectricity. International Journal of Solids and Structures 38, 4439–4461.

Weichen, S., 1997. Rigid line inclusions under anti-plane deformation and in-plane electric field in piezoelectric materials. Engineering Fracture Mechanics 56, 265–274.

Xiao, Z.M., Bai, J., 1999a. On piezoelectric inhomogeneity related problems—Part I: a close-form solution for the stress field outside a circular piezoelectric inhomogeneity. International Journal of Engineering Science 37, 945–959.

Xiao, Z.M., Bai, J., 1999b. On piezoelectric inhomogeneity related problems—Part II: a circular piezoelectric inhomogeneity interacting with a nearby crack. International Journal of Engineering Science 37, 961–976.

Zhong, Z., Meguid, S.A., 1997. Interfacial debonding of a circular inhomogeneity in piezoelectric materials. International Journal of Solids and Structures 34, 1965–1984.